

**COMPUTATIONAL STUDIES OF NATURAL FLAVONOIDS TOWARDS  
THE DISCOVERY OF A POTENTIAL XANTHINE OXIDASE INHIBITOR**

**BELAL OMAR MOHAMMAD ALNAJJAR**

**UNIVERSITI SAINS MALAYSIA**

**2008**

**COMPUTATIONAL STUDIES OF NATURAL FLAVONOIDS TOWARDS THE  
DISCOVERY OF A POTENTIAL XANTHINE OXIDASE INHIBITOR**

**by**

**BELAL OMAR MOHAMMAD ALNAJJAR**

**Thesis submitted in fulfillment of the  
requirements for the degree  
of Master of Science**

**April 2008**

## ACKNOWLEDGEMENTS

In the name of Allah, Most Gracious, Most Merciful *“It is He Who brought you forth from the wombs of your mothers when ye knew nothing; and He gave you hearing and sight and intelligence and affection: that ye may give thanks (to Allah).” Holy Quran 16:78*

First and for most, all praise and thanks to ALLAH. The one whom his decree nothing could happen, and for giving us life to worship him in everything we do during our short lives which we only borrow from him.

I want to thank my supervisors Dr. Habibah A.Wahab, Dr. Nornisah Mohamed and Dr. Rashidah Abdul Rahim for their supports and guidance during my stay in Malaysia and inspiring me with their wisdom and motivation.

Special thanks to: Rashid, Imtiaz, Ismail, Dr. Hassan, Nur Hannani, Sek Peng, Yam Wai Keat, Yee Siew , Suhaini, Fitriah and Sy Bing for their help and the great moments I had during my study at USM. And I will not forget to thank, Osama Arafat, Waleed Rashaideh, Ahmad Makahleh, Asef, Mahmoud Jawarnih, Mohammad Islam, and Tariq my great friends that gave me the true friendship and supported me. Finally, the most special and important people in my life, my parents and my brothers and sisters. I will not forget my mother's loving care and always being there for me even when I was far away from her and her constant prayers for me and guidance in Islam since my childhood. Also my father, for showing me the way and encouraging me in all my endeavours. There is no way no matter what I do in my life to repay them for their love, believing me and giving me the chance.

## TABLE OF CONTENTS

	Page
<b>ACKNOWLEDGEMENTS</b>	ii
<b>TABLE OF CONTENTS</b>	iii
<b>LIST OF TABLES</b>	vi
<b>LIST OF FIGURES</b>	vii
<b>LIST OF SYMBOLS</b>	xii
<b>LIST OF ABBREVIATION</b>	xiv
<b>LIST OF APPENDICES</b>	xvi
<b>ABSTRAK</b>	xvii
<b>ABSTRACT</b>	xix
<b>CHAPTER ONE : INTRODUCTION</b>	
1.1 Statement of the problem	1
1.2 Hyperuricemia	3
1.2.1 Complications of hyperuricemia	6
1.2.2 Therapeutic strategies for preventing the complications	11
1.3 Xanthine oxidase (EC 1.17.3.2)	11
1.3.1 Active site of XO	15
1.3.2 Mechanism of action of XO	17
1.3.3 Mechanism of uric acid production	19
1.4 Flavonoids	24
1.4.1 Biosynthesis of flavonoids in plants	27
1.4.2 Flavonoids as XO inhibitors	30
1.5 Molecular modelling and computational drug design	40
1.6 Molecular mechanics	41
1.7 Molecular docking	50
1.7.1 DOCK 6.0	52
1.7.2 AutoDock 3.0.5	59
1.8 Molecular dynamics (AMBER 8.0)	66
1.9 Aims of the study	76

## **CHAPTER TWO : METHODOLOGY**

2.1	Overview	77
2.2	DOCK 6.0: Rapid filtering of natural flavonoids	79
2.3	AutoDock 3.0.5: Further refinement of the natural flavonoids	81
2.4	AMBER 8.0: Comprehensive studies of the most active flavonoid found by docking studies	83

## **CHAPTER THREE : RESULTS**

3.1	Flavonoids filtering using DOCK 6.0	90
3.2	Further refinement from AutoDock 3.0.5 molecular docking	97
3.2.1	Binding site	102
3.2.2	Hydrogen bond	105
3.2.3	Hydrophobic interaction	110
3.2.4	Aromatic interaction	114
3.2.5	Interaction with Arginine 880	118
3.3	Molecular dynamics results	122
3.3.1	System stability	122
3.3.2	Cluster analysis	129
3.3.3	Hydrogen bond and water mediating hydrogen bond	133
3.3.4	Other non-bonded interactions	137
3.3.5	Free energy of binding calculation	147

## **CHAPTER FOUR : DISCUSSION**

4.1	Flavonoids filtering using DOCK 6.0 and AutoDock 3.0.5	149
4.2	Binding site	152
4.3	Hydrogen bonds	154
4.4	Hydrophobic interaction	157
4.5	Aromatic interaction	160
4.6	Interaction with Arginine 880	162
4.7	Free energy of binding	164

## **CHAPTER FIVE : CONCLUSION AND FUTURE WORK**

5.1	Conclusion	170
5.2	Future work	172
5.3	Concluding remark	173

<b>REFERENCES</b>	174
-------------------	-----

## **APPENDICES**

I	List of Flavonoids used in this study	191
II	DOCK 6.0 input parameters	196
III	Molybdenum's parameter calculation	197
IV	FORTRAN program to calculate molybdenum's parameters	200
V	GPF and DPF input parameter files for AutoDock	204

## LIST OF TABLES

	Page	
1.1	Flavonoids categories	26
1.2	IC <sub>50</sub> and K <sub>i</sub> for some flavonoids (Nagao, <i>et al.</i> 1999)	34
1.3	IC <sub>50</sub> values for a group of flavonoids (Van Hoom <i>et al.</i> 2002)	36
1.4	K <sub>i</sub> values and inhibition type defined by Lin <i>et al.</i> for selective flavonoid compounds and allopurinol	39
2.1	The partial charges for all atoms in quercetin.	85
2.2	The partial charges for all atoms in licoisoflavone-A	86
3.1	DOCK 6.0 energy results, with the inhibition constants (K <sub>i</sub> ) and the concentration of the compound that inhibits 50% of the enzyme (IC <sub>50</sub> ) obtained from literature	93
3.2	Free energy of binding, lowest docked energy and the inhibition constant K <sub>i</sub> calculated by AutoDock 3.0.5 for the 35 top ranked flavonoids obtained from Dock 6.0	100
3.3	Comparison between the amino acids of the binding site for each flavonoid and Salicylate.	103
3.4	The hydrogen bond interactions between the selected flavonoids and XO amino acids.	106
3.5	Summary of amino acids that contribute in hydrophobic interactions	113
3.6	Average (Av.) distance, angle and occupancy (%) of hydrogen bonds between licoisoflavone-A (lic-A) and quercetin (Qur) with XO binding site.	134
3.7	Average (Av.) distance, angle and occupancy (%) of water mediating hydrogen bond for licoisoflavone-A (Lic-A) and quercetin (Qur) with Arg 880 and Glu 1261, respectively	135
3.8	Results of free energy calculation by MM-PBSA for licoisoflavone-A and quercetin, all the energies are in Kcal/mol	148

- 4.1 Comparison between residues found in AMBER 8.0 and in AutoDock 3.0.5 for licoisoflavone-A and quercetin. Residues in bold are the residues that can be seen in both softwares and both ligands.

159



## LIST OF FIGURES

	Page
1.1 Schematic diagram for purine catabolism pathway. XO is xanthine oxidase, GMP is guanosine monophosphate, AMP is adenosine monophosphate, ADP is adenosine diphosphate, ATP is adenosine triphosphate and IMP is inosine 5'-monophosphate	5
1.2 Role of uric acid in the inflammation of gout	7
1.3 Crystal structure of bovine milk XO (1FIQ) from Protein Data Bank (entry code: 1FIQ)	14
1.4 Amino acid residues that contribute in the catalytic reaction in the active site	16
1.5 Basic skeleton for flavonoids	25
1.6 Biosynthesis of chalcones	28
1.7 A schematic presentation of the flavonoid biosynthetic pathway	29
1.8 Types of inhibition. E, S, I are enzyme, substrate and inhibitor, respectively. (a) Competitive inhibition. (b) Non-competitive inhibition. (c) Uncompetitive inhibition	32
1.9 The main features responsible for xanthine oxidase inhibition activity	39
1.10 MM force fields, (a) bond stretching, (b) angle bending, (c) torsional rotation and (d) is the non-bonded interaction (VDW, ELE and HB)	43
1.11 Change of the bond energy as a function of the bond length	46
1.12 Change of the energy as a function of the Angle bending	46
1.13 Variation in torsional energy with H-C-C-H torsion angle (as exemplified by ethane)	46

1.14	Van der Waal interaction, in which $\epsilon$ is the well depth energy, $\sigma_{ij}$ is the distance between atom $i$ and $j$ when the energy is zero, $R_{eqij}$ is the distance between atom $i$ and $j$ at equilibrium, and $R_{ij}$ is the distance between atom $i$ and $j$	48
1.15	The “anchor-and-grow” conformational search algorithm	54
1.16	Periodic Boundary conditions in three directions. When $i$ leaves the central box a its neighbor images will move in the same way	69
1.17	The use of $R_{CUT}$ to reduce and limit the calculation of the interactions of particle $i$ with neighbour particles	71
1.18	Two dimensional view of simulation cell replicated in the three directions of space. The cell marked out by a dotted line, overlapping with cells a,d,e and f symbolises minimum image convention	71
2.1	Flow of the study	78
3.1	Electrostatic (ES) and van der waals (VDW) interaction energies obtained from DOCK 6.0	92
3.2	Surface representation of XO binding site showing the binding mode of salicylate-XO complex. The crystal structure obtained from X-ray colored in blue and docked conformation obtained from AutoDock 3.0.5 in red	101
3.3	The binding conformation of Iicoisoflavone-A (green) and quercetin (red), which appear that they superimposed with salicylate (yellow)	104
3.4	Binding of erysubin-F(green) and papyriflavonol-A(red) are far from salicylate (yellow), Figure shows different amino acids participating in interaction , blue are aminoacids that interact with salicylate and White with eryubin-F and papriflavonol-A	104
3.5	Hydrogen bond interactions between crystal structure of salicylate (stick representation) with Arg 880 and Thr 1010 displayed by ball-and-stick representation found in the binding site	107
3.6	Hydrogen-bonds interaction formed between licoisoflavone-A and Glu 802, Glu 1261 and Thr 1010	107

3.7	Quercetin hydrogen bonds interaction with Asn 768, Ser 876 and molybdopterin co-factor	108
3.8	Hydrogen bond interaction between erysubin-F and Glu 802 and Gln1016	108
3.9	Hydrogen bond interaction between papyriflavonol-A and Lys 771 and Asp 872	109
3.10	LigPlot representation describing the hydrophobic interaction of salicylate in the active site	111
3.11	LigPlot representation describing the hydrophobic interaction of papyriflavonol-A in the active site	111
3.12	LigPlot representation describing the hydrophobic interaction of erysubin-F in the active site	112
3.13	LigPlot representation describing the hydrophobic interaction of licoisoflavone-A in the active site	112
3.14	LigPlot representation describing the hydrophobic interaction of quercetin in the active site	113
3.15	The $\pi$ - $\pi$ stacking of salicylate with Phe 1009 and 914	115
3.16	The $\pi$ - $\pi$ stacking of licoisoflavone-A and Phe 1009 and 914	115
3.17	The $\pi$ - $\pi$ interaction between quercetin and Phe 1009 and 914	116
3.18	The $\pi$ - $\pi$ interaction between erysubin-F and Phe 1013	116
3.19	The $\pi$ - $\pi$ interaction between papyriflavonole-A and Phe 1013 and 649	117
3.20	The distance between the carboxylate of Salicylate and the guanidinium group from Arg 880, the positively charged residues are colored by blue, red for negatively charge and white for neutral residues	119
3.21	Electrostatic interaction between licoisoflavone-A and guanidinium group of Arg 880, the positively charged residues are colored by blue, red for negatively charge and white for neutral residues	119

3.22	Electrostatic Interaction of hydroxyl groups on quercetin and guanidinium group, the positively charged residues are colored by blue, red for negatively charge and white for neutral residues	120
3.23	Electrostatic surface representation of erysubin-F within the active site, the positively charged residues are colored by blue, red for negatively charge and white for neutral residues. Erysubin-F is binding away from the positively charged residues and binding near to neutral residues	120
3.24	Electrostatic surface representation of papyriflavonol-A within the active site, the positively charged residues are colored by blue, red for negatively charge and white for neutral residues. Papyriflavonol-A is binding away from the positively charged residues and binding near to neutral residues	121
3.25	Temperature profile for a) licoisoflavone-A and b) quercetin	124
3.26	Licoisoflavone-A pressure profile during a)the first 80 ps and b) 4ns	125
3.27	Quercetin pressure profile during a)the first 80 ps and b) 4ns	126
3.28	Energy profile for a) licoisoflaone-A and b) quercetin, the green line is the kinetic energy, the black line is the total energy while the red line represents the potential energy	127
3.29	RMSDs of the protein backbone with respect of the crystal structure of XO. a) licoisoflavone-A and b) quercetin	128
3.30	Superimpose the crystal structure of XO (blue) and the most populated structure from molecular dynamics (red) for the two complexes a) licoisoflavone-A-XO and b) quercetin-XO	131
3.31	Comparison of the orientation between docked structure using AutoDock3.0.5 (green) and the most populated structure from MD (yellow) for a) licoisoflavone-A and b) quercetin	132
3.32	WAT 15689 is responsible ion mediate hydrogen bond between the oxygen number 2 of licoisofflavone-A and Arg 880	136

3.33	WAT 14937 is responsible to mediate a hydrogen bond between hydrogen number 6 of quercetin and Glu 1261	136
3.34	Ball and stick representative conformation obtained from cluster analysis for XO-licoisoflavone-A complex. The Figure shows the two phenylalanine residues, Phe 914 and Phe 1009, that form $\pi$ - $\pi$ interaction with ring A and C of licoisoflavone-A	138
3.35	Distance variation between licoisoflavone-A ring A and C and Phe 1009 and 914 during 4 ns simulation	139
3.36	Ball and stick representative conformation obtained from cluster analysis for XO-quercetin complex. The Figure shows the two phenylalanine residues, Phe 914 and Phe 1009, which form $\pi$ - $\pi$ interaction with ring B of quercetin	140
3.37	Distance variation between quercetin ring B and Phe 1009 and 914 during 4 ns simulation	141
3.38	LigPlot representation of the hydrophobic interaction between licoisoflavone-A and the binding site amino acids	143
3.39	LigPlot representation of the hydrophobic interaction between quercetin and the binding site amino acids	144
3.40	Ball and stick representation of the binding of licoisoflavone-A near to Arg 880	145
3.41	Distance between the centre of mass of guanidinium group and O5 of licoisoflavone-A	145
3.42	Ball and stick representation of the binding of quercetin near to Arg 880	146
3.43	Distance between the centre of mass of guanidinium group and O4 of quercetin	146
4.1	The chemical structures of the hit compounds obtained from AutoDock 3.0.5	151

## LIST OF SYMBOLS

$\Sigma$	Sum
$E_{bond}$	Energy contribution that describe bonded term due to bond stretching
$E_{angle}$	Energy contribution that describe bonded term due to angle bending
$E_{torsion}$	Energy contribution that describe bonded term due to dihedral torsions
$E_{ELE}$	Energy contribution that describe electrostatic interaction
$E_{VDW}$	Energy contribution that describe van der waals interaction
$E_{HB}$	Energy contribution that describe hydrogen bond interaction
$K_b$	The force constant or spring strength
$r_0$	The equilibrium bond length
$r_{ij}$	The distance between atom i and j
$\Theta$	The angle between three atoms
$K_{\Theta}$	Constant of the valence angle
$\Theta_0$	Equilibrium valence angle
$\omega$	Torsion angle
$V_n$	Height of the barrier to rotation about the torsion angle
$\gamma$	Phase factor
$\epsilon$	The well depth energy
$\sigma$	The separation distance in which the energy is zero
$q_i$	The partial charges on atoms i
$q_j$	The partial charges on atoms j
$\epsilon_0$	The dielectric constant
$A_{ij}$	VDW parameter for the repulsion force
$B_{ij}$	VDW parameter for the attraction force
$\Delta G_{binding}$	The free energy of binding
$\Delta G_{VDW}$	The free energy of binding for van der waals interaction
$\Delta G_{ELE}$	The free energy of binding for electrostatic interaction
$\Delta G_{HB}$	The free energy of binding for hydrogen bond interaction

$\Delta G_{torsion}$	The free energy of binding for restriction of internal rotors and global rotation and translation
$\Delta G_{desolv}$	The desolvation free energy of binding
$S, \delta$	Atomic solvation parameters
$V$	Volume of the atom
$F$	The force
$a$	The acceleration
$m$	mass
$T$	Temperature in Kelvin
$\Delta S$	Entropy
$\Delta G_{vac}$	The free energy of binding in vacuum (gas-phase)
$\Delta G_{non-polar}$	The non-polar contributions in the free energy of binding
$\phi(r)$	Electrostatic potential
$\rho(r)$	The molecular charge distribution
$\kappa$	Debye-Huckel parameter

## LIST OF ABBREVIATION

Å	Angstrom
Ala	Alanine
AMBER	Assisted Model Building and Energy Refinement
Arg	Arginine
Asn	Asparagine
Asp	Aspartic acid
BPTI	Bovine Pancreatic Trypsin Inhibitor
CHARMm	Chemistry at HARvard Macromolecular Mechanics
Cys	Cysteine
CVFF	Consistent Valence Force Field
DPF	Dock parameter file
EF	Enrichment factor
ELE	Electrostatic
EP	Evolutionary programming
FAD	Flavine adenine dinucleotide
GA	Genetic algorithm
Gln	Glutamine
GPF	Grid parameter file
GROMOS	GRONingen MOlecular Simulation package
Glu	Glutamic acid
Gly	Glycine
HB	Hydrogen bond
His	Histidine
IC <sub>50</sub>	The concentration of the inhibitor that is required for 50% inhibition of the enzyme in vitro
Ile	Isoleucine
K <sub>i</sub>	Inhibition constant
Leu	Leucine
LGA	Lamarckian genetic algorithm
LS	Local search method
Lys	Lysine



MD	Molecular dynamics
Met	Methionine
MM/PBSA	Molecular Mechanics-Poisson Boltzmann Surface Area
NA	Not applicable
ND	Not determined
NPT	Constant number of particles (N), pressure (P) and temperature (T) ensemble
ns	nanoseconds
NVT	Constant number of particles (N), volume (V) and temperature (T) ensemble
NVE	Constant number of particles (N), volume (V) and total energy (E) ensemble
pbc	Periodic Boundary Condition
Phe	Phenylalanine
Pro	Proline
ps	Picoseconds
$R_{cut}$	Cut-off distance
RMSD	Root mean square deviation
ROS	Reactive oxygen species
SA	Simulating annealing
Ser	Serine
Thr	Threonine
Tyr	Tyrosine
Val	Valine
VDW	Van der Waal
XO	Xanthine oxidase

## LIST OF APPENDICES

	Page
I List of Flavonoids used in this study	191
II DOCK 6.0 input parameters	196
III Molybdenum's parameter calculation	197
IV FORTRAN program to calculate molybdenum's parameters	200
V GPF and DPF input parameter files for AutoDock	204

# KAJIAN PENGKOMPUTERAN KE ATAS FLAVONOID SEMULAJADI KE ARAH PENEMUAN PERENCAT XANTINA OKSIDASE

## ABSTRAK

Xantina oksidase (XO) memungkinkan penukaran hipoxantina kepada xantina dan seterusnya xantina kepada asid urik. Peningkatan paras asid urik di dalam serum darah dikenali sebagai hiperurisemia boleh menyebabkan komplikasi seperti sakit sendi dan batu karang. Allopurinol telah diperkenalkan pada tahun 1966, merupakan ubat yang paling berkesan untuk merencatkan aktiviti XO, seterusnya mengurangkan kepekatan asid urik dalam darah. Namun demikian, allopurinol memberi beberapa kesan sampingan yang serius terhadap pesakit, dan kadang-kala boleh membawa maut. Oleh itu, usaha pencarian inhibitor baru yang memberikan kesan sampingan yang rendah tetapi beraktiviti tinggi amatlah diperlukan dengan segera. Inhibitor yang berpontensi mungkin boleh diperolehi daripada sumber semulajadi, seperti flavonoid, di mana ia banyak digunakan dan telah menunjukkan aktiviti perencatan terhadap XO.

Kajian ini bertujuan untuk menyelidik potensi flavonoid sebagai inhibitor XO. Peringkat pertama dalam kajian ini melibatkan penapisan perpustakaan flavonoid yang mengandungi sejumlah 125 sebatian, dengan menggunakan perisian pendokkan molekular DOCK 6.0. Seterusnya AutoDock 3.0.5 digunakan untuk mengkaji 35 flavonoid yang menduduki kedudukan teratas dalam DOCK 6.0. Likoisoflavone-A yang diekstrak daripada akar *Glycyrrhiza glabra Leguminosae* (liquorice) mempunyai aktiviti yang paling tinggi terhadap perencatan XO.

Untuk lebih memahami interaksi di antara flavonoid dan XO, simulasi dinamik molekular telah dijalankan. Sistem pertama melibatkan inhibitor berpotensi yang berada di kedudukan teratas daripada pengiraan pendokkan contohnya likoiso flavone-A dan sistem kedua ialah quercetin dimana ia telah dikenalpasti mempunyai aktiviti “perencatan bersaing” terhadap XO. Daripada trajektori simulasi dinamik, MMPBSA telah digunakan untuk mengira afiniti pengikatan untuk dua ligan tersebut terhadap XO. Keputusan yang diperolehi menunjukkan korelasi yang baik dengan keputusan daripada AutoDock 3.0.5 dan DOCK 6.0. Ini menunjukkan likoiso flavone-A mungkin mempunyai potensi yang tinggi untuk merencat XO. Kajian juga menunjukkan interaksi hidrofobik memainkan peranan penting untuk menghasilkan pengikatan yang lebih baik di antara flavonoid dan XO. Peningkatan bilangan karbon alifatik ke atas struktur flavonoid dapat meningkatkan tahap kehidrofobikan molekul ini. Walaubagaimanapun, kriteria ini tidak semestinya dapat meningkatkan aktiviti perencatan kerana rantainya yang panjang mungkin menghalang ligan untuk dimuatkan ke dalam tapak aktif seperti dalam kes erysubin-F dan papiriflavonol-A.

# COMPUTATIONAL STUDIES OF NATURAL FLAVONOIDS TOWARDS THE DISCOVERY OF A POTENTIAL XANTHINE OXIDASE INHIBITOR

## ABSTRACT

Xanthine oxidase (XO) catalyses the conversion of hypoxanthine to xanthine and subsequently xanthine to uric acid. The increase of uric acid level in blood serum, which called hyperuricemia, can lead to major complications such as gout and kidney stones. Allopurinol that was introduced in 1966 is the most effective drug to inhibit xanthine oxidase activity, thus lowering uric acid concentration. However, allopurinol exhibits severe side effects that sometimes can also lead to death. Therefore, there is an urgent need to discover a new inhibitor which has low side effects but high activity. Potential inhibitor may comes from natural sources, such as flavonoids which have been consumed in abundance that appear to show an inhibitory activity toward XO.

The current study aims to investigate the potency of flavonoids as XO inhibitors. The primary stage of the study involved filtering of a library of flavonoids containing 125 compounds using molecular docking software, DOCK 6.0. Subsequently, AutoDock 3.0.5 was used to further investigate the top 35 ranked flavonoids obtained from DOCK 6.0. Licoisoflavone-A, which is extracted from the root of *Glycyrrhiza glabra Leguminosae* (Liquorice) shows the most potent activity toward the inhibition of XO.

In order to understand the interaction between flavonoid and XO, molecular dynamics simulations were performed. The first system involved potential inhibitor that rank first in the docking calculations i.e. licoisoflavone-A, and the second system included quercetin as it is known to have competitive inhibitory activity on XO. From MD trajectories, MMPBSA was performed to calculate the binding affinities for the two ligands toward XO. The results correlated well with the findings from AutoDock 3.0.5 and DOCK 6.0. This indicates that licoisoflavone-A, might have high potential activity to inhibit XO. It has also been observed that the hydrophobic interactions make important contributions to improve binding between flavonoids and XO. Increasing the aliphatic carbons on the flavonoid structure has increased the hydrophobicity of the compound. Nevertheless, this criteria might not necessarily increase the inhibitory activity, as the long chain might prevent the ligand to fit into the active site, as with the case of erysubin-F and papyriflavonol-A.

# CHAPTER ONE

## INTRODUCTION

### 1.1 Statement of the problem

Xanthine oxidase (EC 1.17.3.2, XO) plays a key physiological role in the metabolism of purines which catalyse the hydroxylation reaction of hypoxanthine to xanthine, and subsequently xanthine to uric acid (Borges *et al.*, 2002; Hille, 1996). Increase in the production of uric acid or decrease in the excretion will lead to increase in the uric acid levels in the body. The increase of uric acid levels in blood is called hyperuricemia (Sitori, 2000). Hyperuricemia leads to many complications such as gout and kidney stones. It may also be associated with renal insufficiency and cardiovascular diseases (Nakagawa *et al.*, 2006). Hyperuricemia is identified when uric acid concentration is  $\geq 7$  mg/dl for men and  $\geq 6$  mg/dl for women (Schlesinger and Schumacher, 2002).

Allopurinol (4-hydroxypyrazolo [3,4-d] pyrimidine), an analogue of hypoxanthine, is a specific potent inhibitor and substrate for XO (Fields *et al.*, 1996). It has been used to treat individuals suffering from hyperuricemia of gout. This drug is slowly oxidized to oxypurinol, a xanthine analogue, which is a more potent XO inhibitor. The most common adverse effects of allopurinol include hypersensitivity reactions, skin rashes and gastrointestinal distress. However, these effects always occur in individuals with reduced glomerular filtration. Syndromes of allopurinol toxicity including rashes, fever, worsening of renal insufficiency, vasculitides, eosinophilia and death have been reported (Bouloc *et al.*,

1996; Horiuchi *et al.*, 2000). These syndromes appear to be more common in the elderly patients with renal insufficiency. Moreover, safety in children and during pregnancy has not been established (Borges *et al.*, 2002). Thus, there is an urgent need to discover compounds with XO inhibitory activities but devoid of the undesirable effects of allopurinol. One potential source of such compounds is medicinal materials of plant origin which are used to treat conditions similar to gouty arthritis.

Flavonoids belong to a group of natural substances with variable phenolic structures and are found in fruit, vegetables, grains, bark, roots, stems and flowers. Researches on flavonoids have suggested these compounds might act as active inhibitors for XO (Cos *et al.*, 1998). Thus, the aim of this study is to investigate the potency of natural flavonoids, as XO inhibitors, using molecular modelling techniques.

Molecular modelling approach has become a major part of rational drug design. Traditional drug design cycle to introduce active compounds is considered too slow and costly. Recently, new methods of processing very large libraries of potentially bioactive small molecules through molecular modelling methods have constantly played an important role in drug discovery. It is hoped that new inhibitors of XO will be discovered by using molecular modelling techniques such as molecular docking and molecular dynamics simulations.



## 1.2 Hyperuricemia

Hyperuricemia is defined when serum uric acid levels exceed 7 mg/dl for men and 6 mg/dl for women. Uric acid is the final product of purine metabolism and these catabolic steps are catalysed mainly by XO enzyme as shown in Figure 1.1. During catabolism, hypoxanthine will be oxidized to xanthine and further to uric acid, which cannot be further metabolised and will be eliminated through the gut and the kidneys (Mandell, 2002; Luk and Simkin, 2005).

Hyperuricemia can be caused by overproduction of uric acid or insufficient excretion by kidneys. Some of the causes that increase the uric acid productions are:

- i- High purine diet (e.g. meat, seafood, alcohol)
- ii- Cytotoxic therapy (i.e. drugs and radiotherapy)
- iii- Myocardial infarction
- iv- Specific enzyme defects

Insufficient uric acid excretion from kidneys can arise from different reasons such as, alcohol intake, drugs (e.g. diuretics) and renal failure. In addition, estrogen is another factor which is believed to promote uric acid excretion in the urine, which explains why men have high risk of developing hyperuricemia compared to women. However, involvement of more than one factor has been reported such as a combination of overproduction and low excretion of uric acid, high alcohol consumption and Glucose-6-phosphatase deficiency, indicating that

hyperuricemia is a multifactorial disorder leading to a complicated diseases like gout urolithiasis (Dincer *et al.*, 2002). As these factors are suspected in high percentage in adults, 10% of adults are documented to have hyperuricemia at least once in their life. Therefore, it is worth to look for an agent/s which participates in alleviating or preventing this common disorder (Hayden and Tyagi, 2004). In the following paragraphs an overview on complications caused by hyperuricemia in order to understand the principal factors behind these disorders and then looking for the possible treatment targets will be presented.

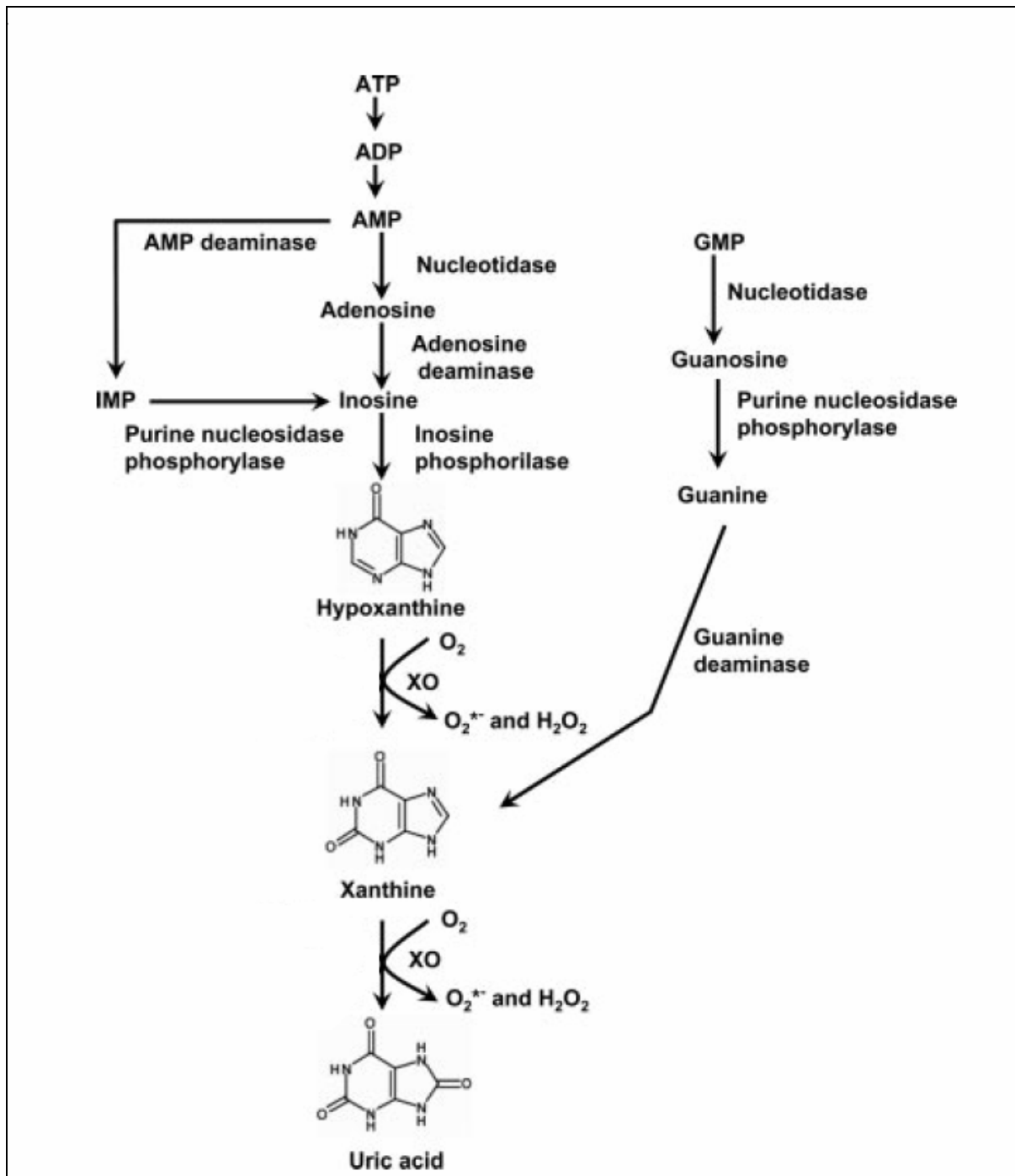


Figure 1.1: Schematic diagram for purine catabolism pathway. XO is xanthine oxidase, GMP is guanosine monophosphate, AMP is adenosine monophosphate, ADP is adenosine diphosphate, ATP is adenosine triphosphate and IMP is inosine 5'-monophosphate

### **1.2.1 Complications of Hyperuricemia**

The major complications of hyperuricemia are gout, urolithiasis, reactive oxygens production and acute uric acid nephropathy. In addition to that, some diseases are frequently seen with elevated uric acid concentration such as cardiovascular disease, although no direct role has yet been confirmed (Pascual and Pedraz, 2004).

#### **1- Gout**

Gout is a metabolic disorder characterised by high levels of uric acid in the blood (hyperuricemia). This hyperuricemia results in the deposition of crystals of sodium urate in tissues, especially in kidneys and joints. Hyperuricemia does not always lead to gout but gout is always preceded by hyperuricemia. The deposition of urate crystals initiates an inflammatory process involving the infiltration of granulocytes that phagocytize the urate crystals (Figure 1.2). This process generates oxygen metabolites, which damage tissue, resulting in the release of lysosomal enzymes that induce an inflammatory response. In addition, lactate production in the synovial tissue also increases. This will lead to local decrease of pH which further cause more deposition of urate crystals (Mycek *et al.*, 2000).

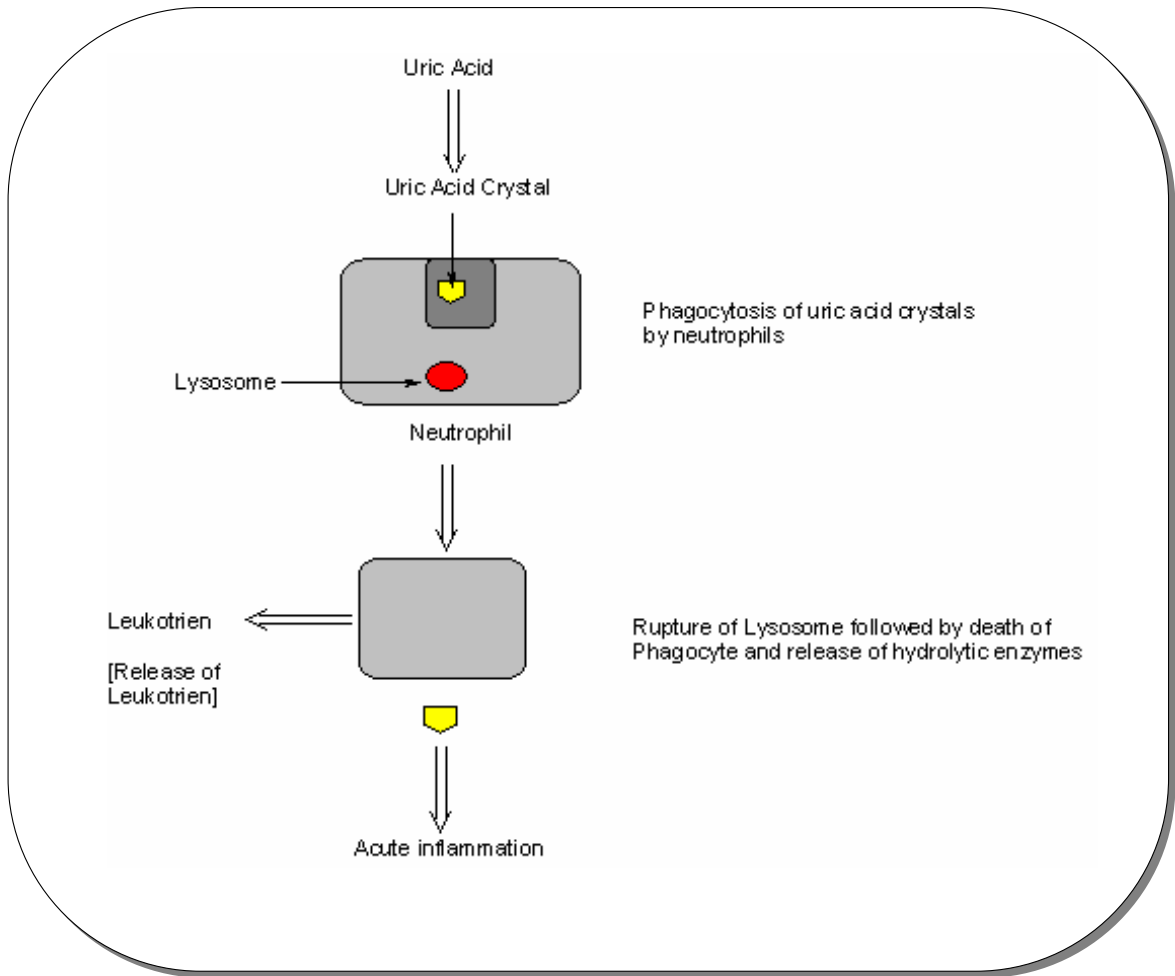


Figure 1.2: Role of uric acid in the inflammation of gout

The diagnosis of gout is based on the presence of monosodium urate crystals in the synovial fluid or tophi (Weselman and Agudelo, 2001). This deposition will exacerbate leading to recurrent episodes of acute arthritis, the classic manifestation of gout. It should be noted that different factors are participating in the development and progress of this diseases as well. The incidence of gout rises dramatically with age. It has been hypothesized that estrogen will act as a protecting agent against urate deposition, by promoting renal excretion of uric acid. Therefore the overall men:women ratio ranged between 7:1 and 9:1. Factors like inherited enzyme deficiencies, obesity, decrease renal function, hypertension and alcohol also play a role (Wright and Pinto, 2003). It has been identified that 20% of gouty patients make renal stones (Foye, 1995).

Understanding all the above mentioned factors and the complicated mechanism will help us in identifying what type of gout we are targeting for the treatment as the treatment of gout depends on the type of attack. Acute gouty attacks therapies mainly include nonsteroidal ant-inflammatory drugs (NSAIDs) or colchicine. Meanwhile, controlling the uric acid level in the blood is still the main target particularly in the management of the chronic attacks. Examples of such drugs are allpurinol, probenecid and sulfinpyrazone (Mandell, 2002; Weselman and Agudelo, 2001).

## 2- Urolithiasis

Urolithiasis is the process of stone formation in kidneys and other urinary ailments. Stone formation is not itself a specific disease, it is much more complicated than that. Urolithiasis is a multifactorial disease and presents a final stage of a complication of many different diseases (Foye, 1995). For stone to be formed, many factors have to be involved however supersaturation of urine with regards to the crystal components from time to time is prerequisite for the crystallization process to be initiated leading to crystal formation and precipitation. Crystals are of different types and one of them is uric acid crystals. There are two types of deposits, one that composed of uric acid and other composed of urate. pH of the urine has been found to influence the availability and solubility of substances. Studies showed that pH will determine the type of deposition, in which acidic media (pH 3.7) is suitable for uric acid deposition while at higher pH (pH 7.4) is suitable for urate deposition (De Vries and Sperling, 1977).

Uric acid stones account for 5-10% of all renal stones in the United States. Not all stones in hyperuricemic patients are composed primarily of uric acid, but uric acid acts as a nidus for the formation of different stones mainly calcium stones (Dincer *et al.*, 2002).

### 3- Reactive Oxygen Species (ROS) Free Radical Production induced by XO

Reactive oxygen species (ROS) include oxygen ions, free radicals and peroxides. ROS are generally very small molecules and are highly reactive due to the presence of unpaired valence shell electrons. During uric acid production pathway, hypoxanthine will be hydroxylised to xanthine and then to uric acid via an enzyme called xanthine oxidase (XO). Enzyme xanthine oxidase produces ROS during the oxidative half reaction, which takes place in the binding of FAD of the reduced form of XO with oxygen molecule. This reaction will lead to transfer of electrons from the reduced form of XO to the oxygen according to following reaction in the Scheme 1.1 (Mondal *et al.*, 2000):



Scheme 1.1

The presence of high quantity of these radicals have been strongly responsible for disturbing cell physiology associated to oxidative stress such as cancer inflammation and arterioscleroses (Da Silva *et al.*, 2004; Van Hoorn *et al.*, 2002)



### **1.2.2 Therapeutic strategies for preventing the complications**

Most of the therapeutic strategies for hyperuricemia focus on lowering uric acid level in the blood below the saturation point, thus preventing the deposition of urate crystals. This can be achieved by interfering with uric acid synthesis via inhibiting XO enzyme e.g. by using allopurinol or by increasing uric acid excretion e.g. using probenecid or sulfinpyrazone (Mycek *et al.*, 2000).

Prevention of conversion of XO to the reduced form will lead to inhibition of ROS formation (Cotelle *et al.*, 1996a). Thus, in this study, the strategy is to inhibit XO as a measure for the management of hyperuricemia. By inhibiting XO activity, uric acid and superoxides production will be ceased.

### **1.3 Xanthine Oxidase (EC 1.17.3.2)**

Xanthine oxidase (XO) is a molybdoflavoenzyme which can be found in almost all species. The human enzyme is widely distributed with the highest levels are in liver and intestine (Parks and Granger, 1986). XO from human breast milk has been purified and characterised successfully in 1986 (Krenitsky *et al.*, 1986). Bovine milk XO is widely available, thus it has been known for 100 years and studied in its pure form for over 60 years, therefore it has been used in most of the studies (Patton and Keenan, 1975). XO has high amino acids sequence homology among the mouse, rat, bovine and human enzymes with about 90% identity, and consisting of about 1,330 amino acids (Nishino, 1994; Borges *et al.*, 2002; Godber

*et al.*, 2005). Studies showed the existence of similar physicochemical properties of XO between human and bovine milk, but it has only approximately 5% of the activity of the bovine milk enzyme towards xanthine and related substrates proposing that the low activity is due to grossly deficient of molybdenum (Abdeh *et al.*, 1992). XO is distributed in most of the tissues, with high levels in liver and intestine. Microscopic studies of cultured human endothelial cells showed that XO is present in cytoplasm and also on the outer surface of the cell membrane (Harrison, 2002).

The X-ray crystal structure of bovine milk XO has been released in the Protein Data Bank ([www.pdb.org](http://www.pdb.org)) in August 2000 with a PDB code entry of (1FIQ) (Enroth *et al.*, 2000). The structure has been used in this study due to X-ray structure availability and similar physicochemical properties with human XO. While the X-ray crystal structure for human XO has been released on May 2007 with a PDB code entry of (2CKJ) (Pearson *et al.*, 2007).

Bovine milk XO enzyme obtained from the protein data bank (PDB entry 1FIQ). The crystal structure is a homodimer of 145 kDa subunits, which consists of a 20-kDa N-terminal domain containing two iron-sulfur centers, a 40-kDa middle domain containing flavine adenine dinucleotide (FAD), and an 85-kDa C-terminal containing the molybdopterin cofactor (Kisker *et al.*, 1998; Mondal *et al.*, 2000; Borges *et al.*, 2002). The monomer can be divided into three domains, the small N-domain starts from residue 1 to 165, and contains both iron/sulfur cofactors that is connected to the second domain (FAD-binding domain) residues 226 to 531 by

segment of residues 166 to 225. FAD also connected to the third domain by another linker composed of residues 532 to 589. The large third domain (residues 590 to 1,332) is the molybdopterin cofactor (Figure1.3) (Enroth *et al.*, 2000).

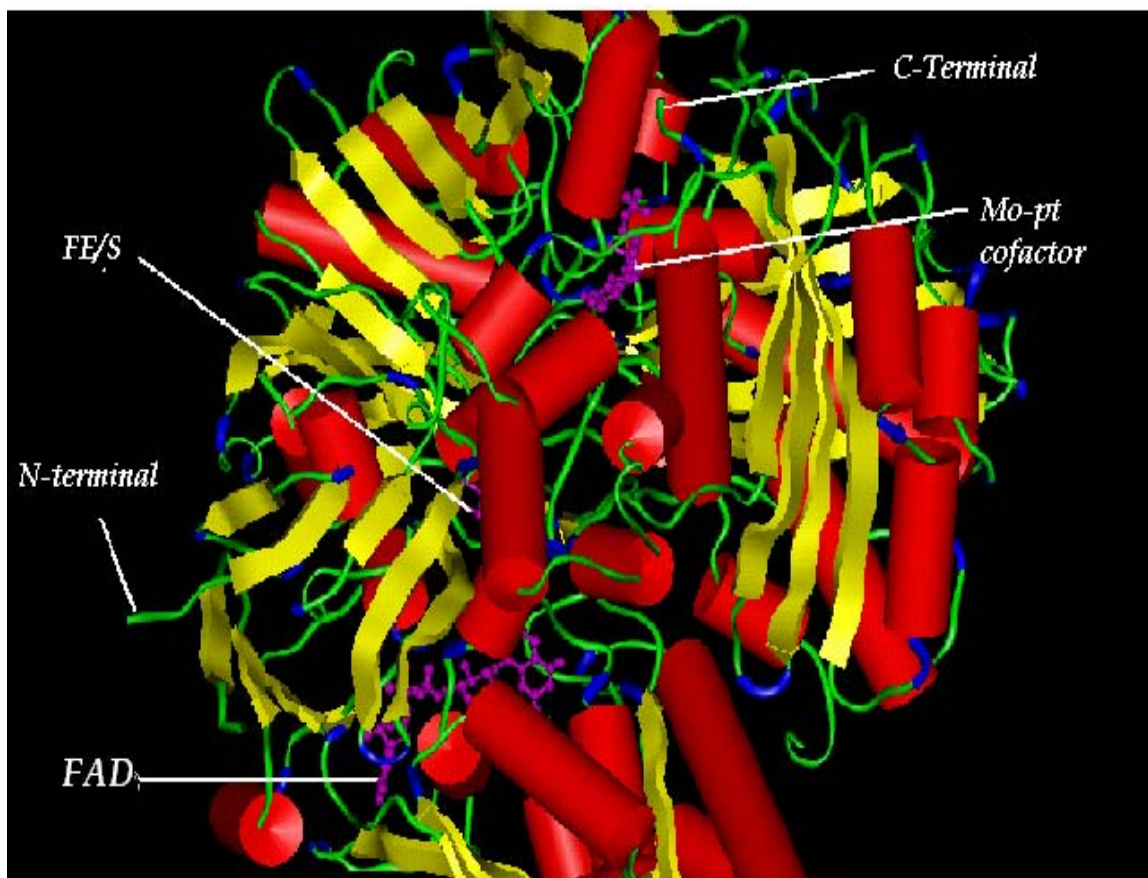


Figure 1.3: Crystal structure of bovine milk XO (1FIQ) from Protein Data Bank (entry code: 1FIQ)

### 1.3.1 Active site of XO

The crystal structures of bovine milk XO suggests that hypoxanthine and xanthine bind to the C-terminal domain of the XO, close to the molybdopterin cofactor. During substrate oxidation, the Mo centre is first reduced by electron received from the substrate and subsequently re-oxidized, as the electron passes first to the iron- sulfur centres and then to the FAD centre, and are finally donated to  $\text{NAD}^+$  or  $\text{O}_2$  (Hille and Nishino, 1995; Kisker *et al.*, 1998; MacMaster and Enemark., 1998). The mechanism of uric acid production will be discussed in Section 1.3.3. Salicylate was crystallised with XO as a competitive inhibitor, which binds to the binding site of the enzyme inhibiting xanthine or hypoxanthine to bind and be metabolised by XO. The amino acid that plays an important role in the catalytic reaction specified by Hille *et al.* (2004) is Glu 1261 (Figure 1.4) (Hille *et al.*, 2004). The enzyme complex with salicylate shows that both the carboxylate atoms are close to the guanidinium group of Arg 880 (3.0 Å and 3.1 Å). An interaction with Glu 1261 can be involved via water 230. Hydrogen bond can be formed between the hydroxyl group of salicylic acid with both amide and hydroxyl side chain of Thr 1010. The aromatic ring of Phe 914 slightly overlaps with salicylic acid ring, on the other hand, salicylate ring forms a T-shape aromatic interaction with Phe 1009 ring (Enroth *et al.*, 2000).

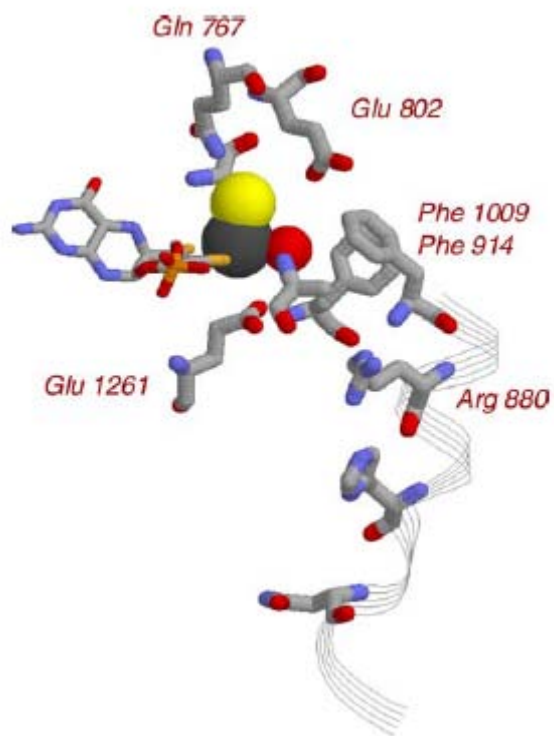
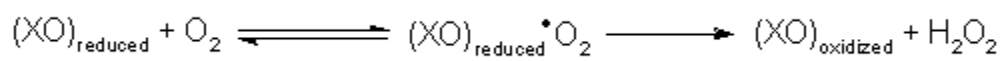


Figure 1.4: Amino acid residues that contribute in the catalytic reaction in the active site

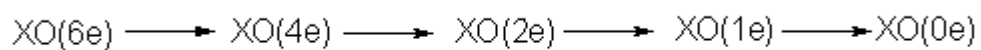
### 1.3.2 Mechanism of action of XO

The reaction of XO composed of two catalytic reactions, reductive half and the oxidative half reaction. The reductive half reaction is the conversion of xanthine to uric acid, which takes place in the molybdenum centre of the enzyme. In this reaction, Mo(VI) is converted to its reduced form Mo(IV). While the oxidative half reaction takes place at the FAD centre, and oxidize Mo(IV) to Mo(VI) by molecular oxygen with the formation of ( $O_2^{\bullet -}$ ) or  $H_2O_2$  (Olson *et al.*, 1974; Huber *et al.*, 1996).

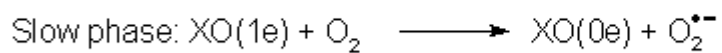
The oxidative part of the reaction involves the binding of molecular oxygen to the FAD centre of the reduced form of XO. This will lead to the transfer of electrons from the reduced form, to achieve enzyme oxidation (Hille and Massey, 1981) as shown in Scheme 1.2. Slow and fast phase in this reaction have been observed, and six electrons are transferred throughout the reaction (Hille and Massey, 1981; Mondal *et al.*, 2000) as shown in Scheme 1.3. The fast phase involves in the transfer of five electrons and the formation of hydrogen peroxide ( $H_2O_2$ ) and superoxide ( $O_2^{\bullet -}$ ). Whereas the slow phase includes the oxidation of one electron and the formation of superoxide only (Mondal and Mitra, 1996) as given in Scheme 1.4. The mechanism of the formation of xanthine and uric acid is considered as the reductive half reaction (Scheme 1.5) (Kim *et al.*, 1996). Further discussion will be presented in the next section.



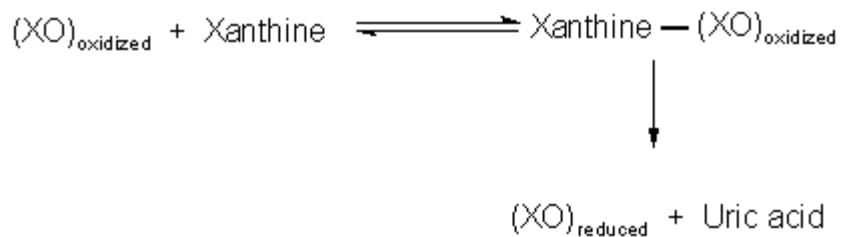
Scheme 1.2



Scheme 1.3



Scheme 1.4



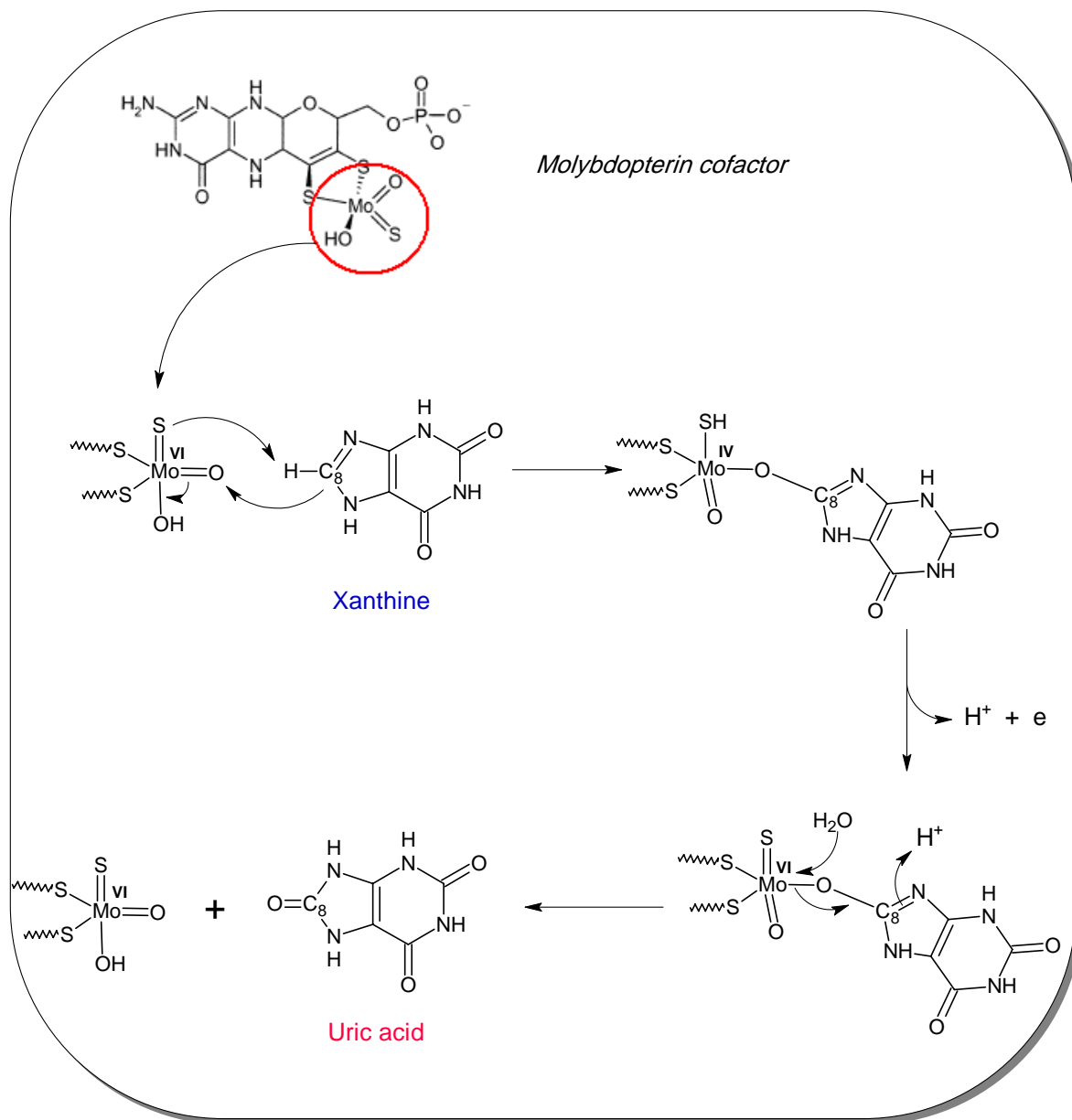
Scheme 1.5



### 1.3.3 Mechanism of uric acid production

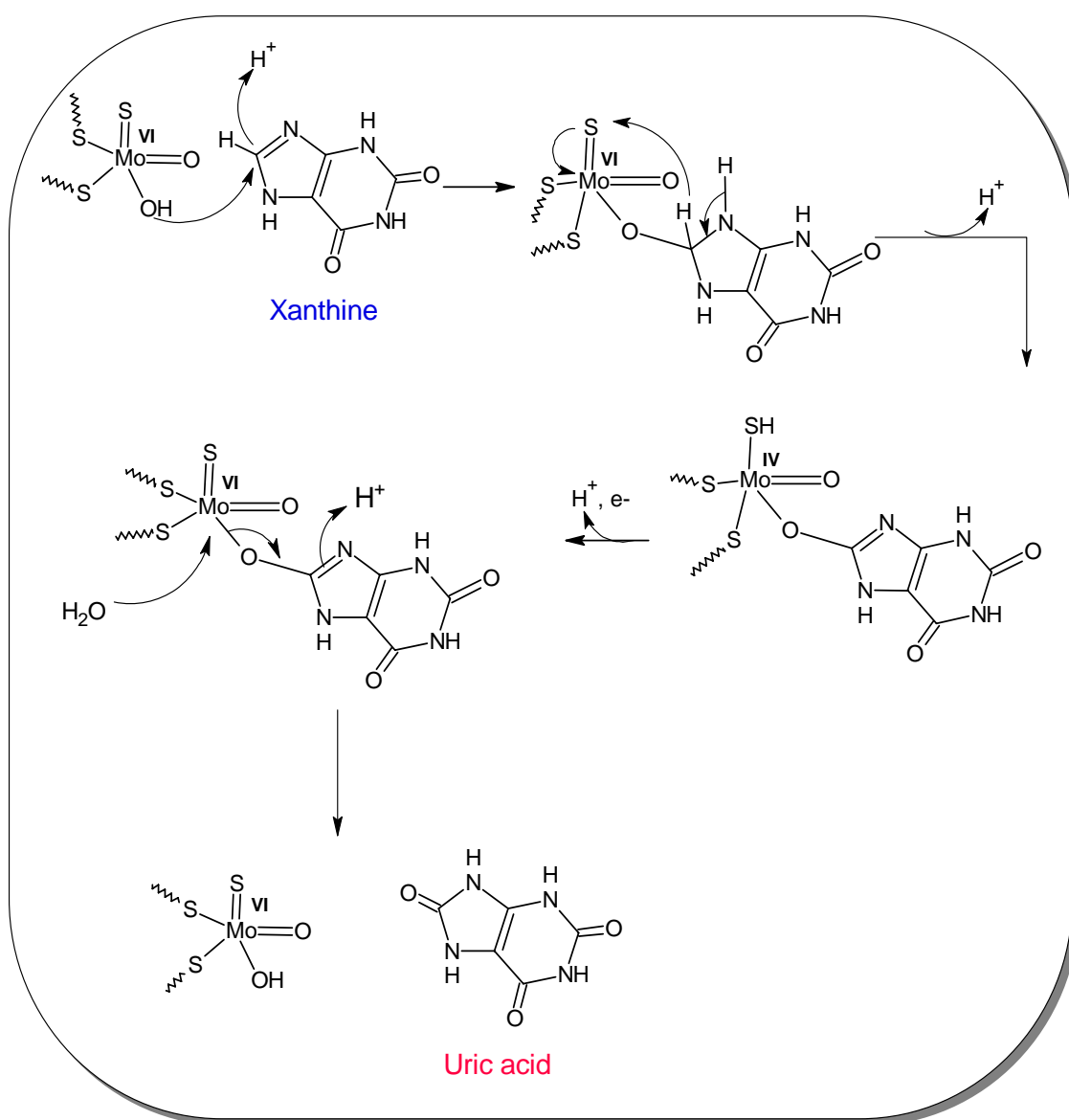
Many researchers studied the catalytic reaction of XO proposing different mechanisms on the source and the way to incorporate the oxygen atom that is used to oxidize the substrate. But they all share the same concept, which is the hydroxylation to C-8 of xanthine.

In the early days of identifying the mechanism, it was proposed that the oxygen source is derived from water (Murray *et al.*, 1966). However, it has been shown later that the oxygen atom incorporated into product is derived from the catalytically labile site of the enzyme, which must then be regenerated with oxygen from water. In addition, it has been suggested that the catalytically labile site of XO is in fact the Mo=O of the enzyme. A mechanism of action has been proposed in which the catalysis proceeds via deprotonation of C-8 position of xanthine, or hypoxanthine, followed by nucleophilic attack of the resultant carbanion on the Mo(VI)=O group to give Mo(IV)-O-R species (Hille and Sprecher, 1987), as shown in Scheme 1.6. The abstraction of C-8 hydrogen by Mo=S group is compatible with the known acidity of this position of xanthine ( $pK_a \sim 14$ ) and the Mo=S is sufficiently basic to protonate upon reduction of the enzyme. Furthermore, it appears that the reaction initiated by hydrogen abstraction followed by carbanion attack on Mo=O is the more likely reaction rather than a hydride attack on Mo=S, which was proposed by Bray and co-workers (Bray *et al.*, 1979).



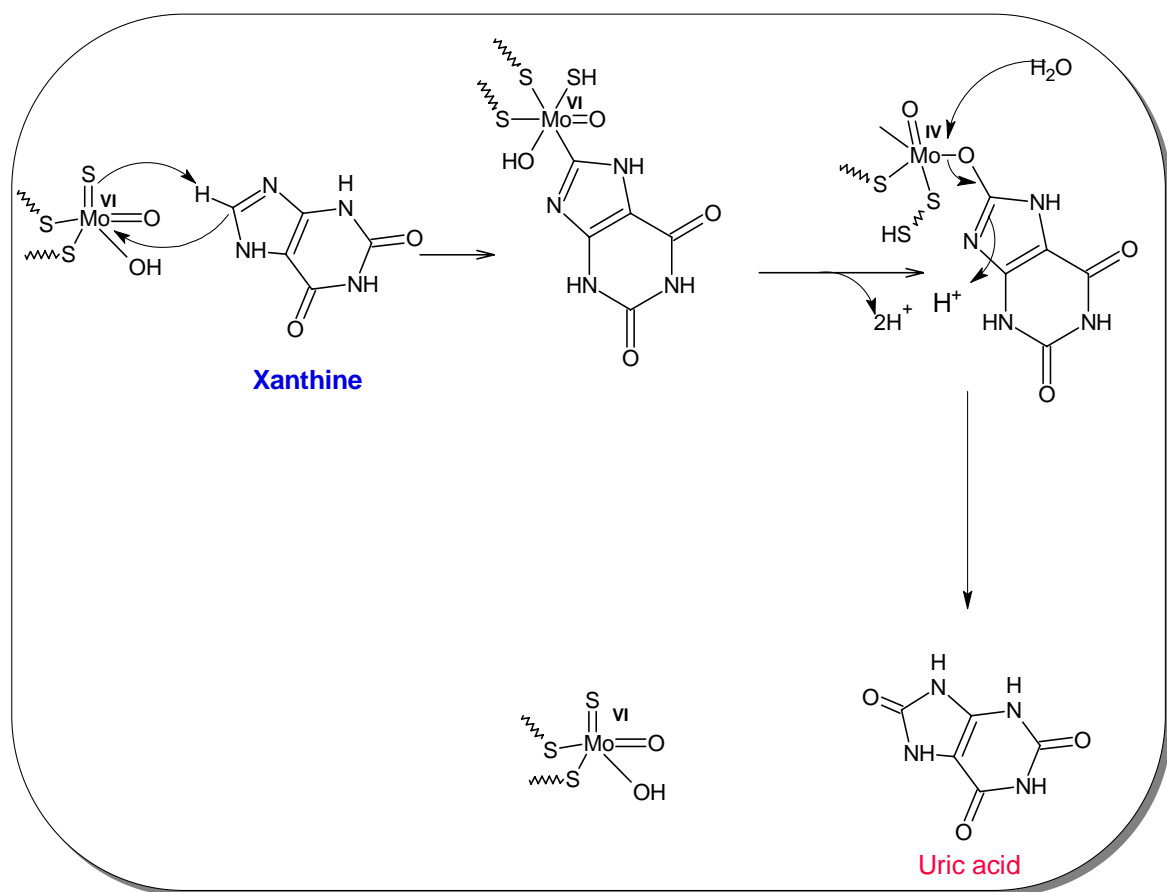
Scheme 1.6

A mechanism involving the metal-coordinate hydroxyl has been proposed for XO mechanism of action (Huber *et al.*, 1996). The reaction is initiated by nucleophilic attack on C-8 of xanthine by the hydroxyl group to give a transient tetrahedral intermediate. This breaks down by hydride transfer to Mo=S group, with resultant reduction of the molybdenum to Mo(IV) valence state. It should be noted that the  $pK_a$  for the C-8 position is also to be relatively low, to be suitable for nucleophilic attack, as specified in Scheme 1.7.



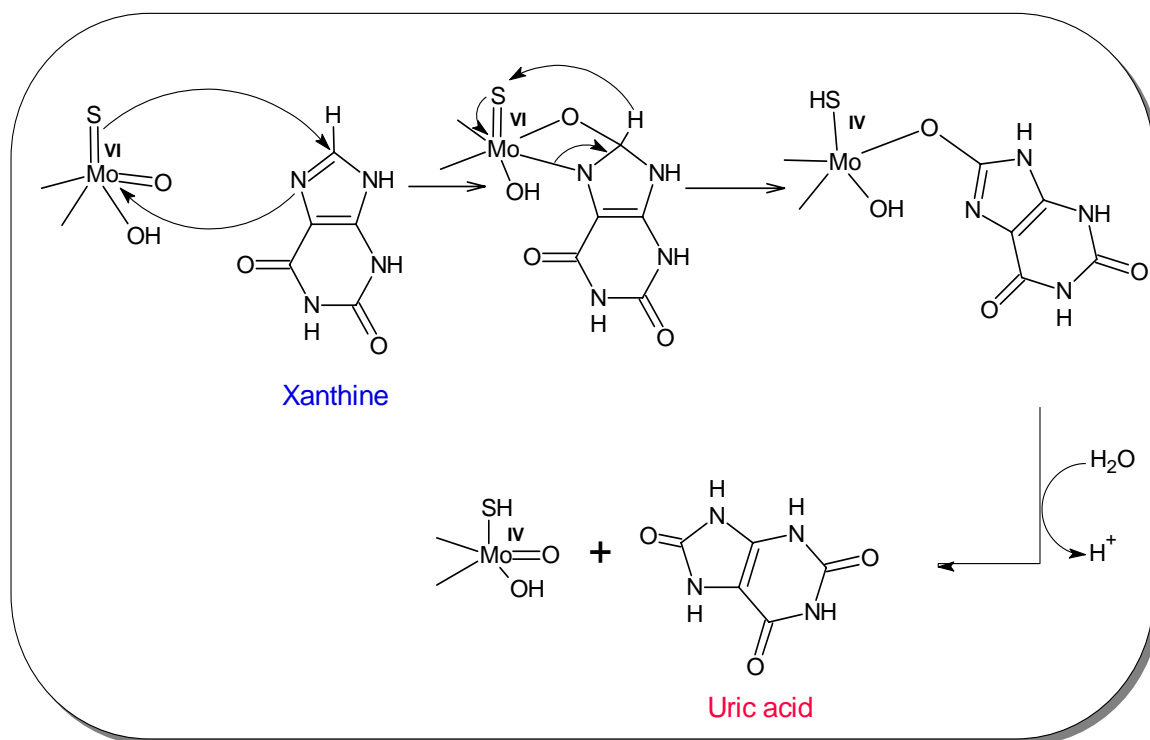
Scheme 1.7

As shown in Scheme 1.8, this mechanism involves the reducing the Mo=S group to Mo-SH by abstracting the hydrogen from C8-H of xanthine, then the formation of molybdenum–C8 bond. This will incorporate hydroxide from solvent to yield the same intermediate as in the previous proposed mechanisms (Coucouvaniis *et al.*, 1991).



Scheme 1.8

Pilato and Stiefel (1993) proposed that N-7/C-8 double bond adds across the Mo=O directly in a cyclo-addition, to give an intermediate that can be broken by hydride transfer to give a species different from that proposed previously. The Mo=O group must be regenerated immediately in the catalytic sequence, and the water molecules can serve such purpose, as given in Scheme 1.9 (Pilato and Stiefel, 1993).



Scheme 1.9

## 1.4 Flavonoids

In nature, flavonoid compounds are products extracted from plants and they are found in several parts of the plants: leaves, fruits, etc. Flavonoids are used by the vegetables for their growth and defence against plagues (Havsteen, 2002). They are a class of low molecular weight phenolic compounds that are widely distributed in the plant kingdom. They constitute one of the most characteristic classes of compounds in higher plants. Many flavonoids are easily recognized as flower pigments in most angiosperm families. However, their occurrence is not restricted to flowers but includes all parts of plant (Dewick, 2001). The chemical structure of flavonoids is based on a C<sub>15</sub> skeleton with two phenolic rings connected together by three carbon units as shown in Figure 1.5. Flavonoids are grouped according to the presence of different substituents on the rings and the degree of ring saturation. They are frequently attached with sugars moiety to increase their water solubility (Stumph and Conn, 1981). Flavonoids have several subgroups, which include chalcones, flavones, flavonols and isoflavones. Table 1.1 shows the main subgroups of flavonoids.

A novel Laureate, Albert Szent-Gyorgyi, Ph.D., who discovered vitamin C, had isolated the flavonoids (proanthocyanidins) in 1930's. He found that flavonoids could strengthen capillary walls that vitamin C cannot. At the beginning, the flavonoids were recognized as vitamin P. Besides that, some chemist also classified flavonoids as a single vitamin. Nowadays, there are about 4,000 flavonoids compounds that contribute to the colorful pigments of fruits, herbs and